

# Highly efficient Er- and Yb - doped $\text{YAl}_3(\text{BO}_3)_4$ laser materials: crystal growth and characterization

V. V. MALTSEV, E. A. VOLKOVA, N. I. LEONYUK<sup>a\*</sup>, N. A. TOLSTIK<sup>a</sup>, N. V. KULESHOV<sup>a</sup>

Department of Crystallography & Crystallization, Geological Faculty, Moscow State University 119991/GSP1  
Moscow, Russian Federation

<sup>a</sup>Institute for Optical Materials and Technologies, Belarus National Technical University, Minsk, Belarus

(Er,Yb): $\text{YAl}_3(\text{BO}_3)_4$  single crystals have been obtained from  $\text{K}_2\text{Mo}_3\text{O}_{10}$  based fluxed melts. Also, 100  $\mu\text{m}$ -thick Yb: $\text{YAl}_3(\text{BO}_3)_4$  crystal layers were grown by liquid phase epitaxy method. Their growth rates varied from 1.5 to 10  $\mu\text{m}/\text{h}$  in the supercooling range of 3–12.5 °C. The room temperature polarized absorption spectra of the layers were recorded and compared with those for Yb: $\text{YAl}_3(\text{BO}_3)_4$  single crystals. Strong and broad absorption bands were observed at 976 nm with a peak absorption coefficient of about 14  $\text{cm}^{-1}$ . The emission lifetime of  $\text{Yb}^{3+}$  ions in both layers and bulk crystals was found to be 480  $\mu\text{s}$ .

(Received September 1, 2008; accepted October 30, 2008)

**Keywords:** Growth from high temperature solutions, Single crystal growth, Liquid phase epitaxy, Borates, Laser materials

## 1. Introduction

To date, various erbium and ytterbium codoped phosphate glasses are mostly used as gain media for solid-state lasers emitting in the eye-safe 1.5–1.6  $\mu\text{m}$  spectral range [1,2]. They are of great potential for range-finding, environmental sensing, aerial navigation, telecommunications, medicine, etc. In these systems short  $^4I_{11/2}$  level lifetime minimizes Er→Yb energy back-transfer, excited state absorption and cross-relaxation losses, whereas high luminescence quantum yield from  $^4I_{13/2}$  level allows to keep low laser threshold. However, glasses exhibit low mechanical stability and thermal conductivity (typically less than 1  $\text{W}/\text{m}^*\text{K}$ ), which limit the output power at the level of about 150–200 mW.

CW room-temperature 1.5-1.6  $\mu\text{m}$  lasing was demonstrated for several Er-doped and Er,Yb-codoped crystals including  $\text{Y}_3\text{Al}_5\text{O}_{12}$  and  $\text{Y}_2\text{SiO}_5$  [3],  $\text{Ca}_2\text{Al}_2\text{SiO}_7$  [4],  $\text{YVO}_4$  [5],  $\text{LaSc}_3(\text{BO}_3)_4$  [6],  $\text{KY}(\text{WO}_4)_2$  [7] etc. In these cases, however, typical output power does not exceed 150 mW in combination with poor slope efficiency. The most efficient diode-pumped laser action among crystalline media has been obtained with Yb,Er-activated oxoborates: 250 mW of CW output power with 26,8 % efficiency for  $\text{YCa}_4\text{O}(\text{BO}_3)_3$  [8] and 158 mW with 14% efficiency for  $\text{GdCa}_4\text{O}(\text{BO}_3)_3$  [9].

In the meantime,  $\text{YAl}_3(\text{BO}_3)_4$  (YAB) crystal is a well-known laser host for Yb and Nd ions [10–11]. Recently Er,Yb:YAB material having high potential of 1.5  $\mu\text{m}$  efficient multiwatt laser action with diode pumping at 980 nm has been demonstrated. CW output power of 1 W with a slope efficiency of 35% was obtained and the output power was limited by available pump source [12-13].

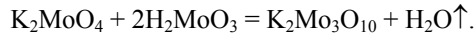
Mode-locked regime has been realized with pulse duration of about 4 ps and average output power of 270 mW [14].

Crystalline thin layers doped with  $\text{Yb}^{3+}$  are very attractive for applications in high-power thin-disk lasers, as well as active waveguide devices, such as planar and channel waveguide lasers. Thus, efficient laser operation of Yb:KY(WO<sub>4</sub>)<sub>2</sub> and Yb:KL<sub>u</sub>(WO<sub>4</sub>)<sub>2</sub> layers with maximum output power of 290 mW and a slope efficiency of 80.4% under laser pumping at 980 nm was demonstrated [15-17]. However, both these tungstate matrices suffer from rather lower thermal conductivity (of about 3  $\text{W}/\text{m}^*\text{K}$ ) in contrast to YAB (4,7  $\text{W}/\text{m}^*\text{K}$  [18]), which being doped with  $\text{Yb}^{3+}$  demonstrates favorable laser properties as well as efficient self-doubling due to high second-order nonlinearity [10].

Here, recent results on the growth of Er,Yb-codoped YAB bulk crystals and Yb:YAB crystalline layers are discussed. Also, data on spectroscopy of these laser materials are reported.

## 2. Experiment

Since YAB is an incongruently melting compound [19],  $\text{Er}_x\text{Yb}_y\text{Y}_{1-x-y}\text{Al}_3(\text{BO}_3)_4$  with  $x = 0.005$  to 0.015 and  $y = 0.07$  to 0.15 in the starting crystalline substances were obtained by dipping seeded solution growth (DSSG) method using  $\text{K}_2\text{Mo}_3\text{O}_{10}$  based fluxes. Concentration of YAB, Yb:YAB and (Er,Yb):YAB in the initial load corresponded to 17 wt.%. Starting chemicals (at least 99.9% and 99.99% purity for rare earths and other materials, respectively) were  $\text{Y}_2\text{O}_3$ ,  $\text{Yb}_2\text{O}_3$ ,  $\text{Er}_2\text{O}_3$ ,  $\text{Al}_2\text{O}_3$  and  $\text{B}_2\text{O}_3$ , but  $\text{K}_2\text{Mo}_3\text{O}_{10}$  was previously sintered of  $\text{K}_2\text{MoO}_4$  and  $\text{H}_2\text{MoO}_4$  at 650 °C according to the scheme:



The starting mixture in Pt crucible of 70 cm<sup>3</sup> volume was placed into a vertical electric furnace equipped with a PROTHERM microprocessor containing controller. The temperature at the crucible bottom was kept 2–3 °C higher than at the melt “mirror”. Before DSSG, the saturation temperatures of fluxed melts were precisely determined by a probe technique, and it was found to be 1060–1080 °C depending on the dopant concentration. A “point” YAB seed of 0.3x0.3x1.0 mm<sup>3</sup> dimension was dipped into fluxed melt. During the crystal growth supersaturation was kept within the temperature interval of 1080–1000 °C by the cooling of fluxed melts in the range of 0.2–5 °C/day following the experimental data on the solubility and crystallization kinetics. At the end of growth process, the crystal was pulled out and cooled to the room temperature within several days.

Yb:YAB epitaxial layers were grown by liquid phase epitaxy (LPE) method on substrates made of pure YAB. Since waveguides efficiency depends on the difference in refractive indices ( $\Delta n$ ) between the substrate and the active layer, these characteristics in pure and Yb-doped YAB single crystals were precisely determined in visible wavelength range [20]. Replacement of Y<sup>3+</sup> by Yb<sup>3+</sup> up to 7 at.% results in increasing of ordinary and extraordinary refraction indices by ~ 0.002 and 0.001 respectively. This is a reason why YAB substrate was chosen at this initial stage of Yb:YAB LPE growth, which can be considered as almost homoepitaxial crystallization in this system. The substrate wafers with sizes up to 0.7–10 mm<sup>2</sup> and thickness of 0.5–2 mm were cut from YAB single crystals parallel to rhombohedron and prism faces and mechanically polished (Fig. 1).

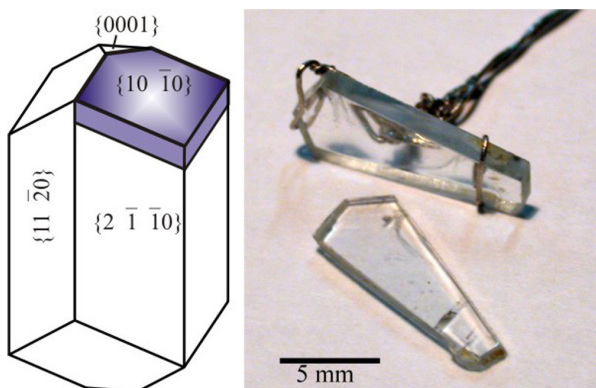


Fig. 1. Wafers cut from YAB single crystal parallel to rhombohedron face.

The thin film growth was performed under similar conditions. At the beginning of epitaxial growth, the YAB substrate was slowly dipped into the solution at the temperature 1 °C higher than saturation point. 10–20 min later, the temperature was lowered by 3–10 °C, and substrate was kept for 9–36 h depending on supercooling of the fluxed melt as well as on expected thickness of the

layer, as it follows from their growth kinetics. Then, the substrate and film grown were pulled out slowly, cooled to the room temperature and released from the crystallized melt by dissolution in hydrochloric acid, distilled water and ethanol.

The composition, homogeneity and morphology of bulk crystals and thin layers were studied by analytical scanning electron microscope JSM-5300+Link ISIS. A Cameca analyzer was used for investigation of layer composition with an accuracy up to 0.02–0.03 wt.%. The effective distribution coefficients ( $K$ ) of Er<sup>3+</sup> and Yb<sup>3+</sup> in (Er,Yb):YAB were calculated using the equation:

$$K = C_{\text{crys}}/C_{\text{diss REYAB}}$$

where  $C_{\text{crys}}$  is rare earth content in grown crystals and  $C_{\text{diss REYAB}}$  is RE concentrations in the borate substances of fluxed melt.

The absorption spectra of crystals and thin films were measured with Cary-5000 spectrophotometer with 0.4 nm spectral resolution. The luminescence kinetics of Er<sup>3+</sup> and Yb<sup>3+</sup> ions in Er(1.5at.%),Yb(11at.%)YAB crystal and Yb(10at.%)YAB thin film were detected using 0.3 m monochromator and InGaAs photodiode after the excitation by Nd-YAG-pulse-pumped optical parametric oscillator (20 ns pulse duration). The laser experiments were performed in a three-mirror cavity using 7W fiber-coupled laser diode as a pump source and 1.5-mm thick Er(1.5at.%),Yb(11at.%)YAB crystal as an active element.

### 3. Results and discussion

#### 3.1. Crystal growth

The visually transparent YAB and (Er,Yb):YAB crystals were obtained with a typical size up to 10x10x15 mm<sup>3</sup> and 8x8x12 mm<sup>3</sup> respectively. YAB crystals are colorless, but the (Er, Yb):YAB samples have the characteristic “erbium” light-pink color. All single crystals have well developed simple crystallographic forms of huntite-type borates [19], namely, two trigonal prisms and rhombohedron (Fig. 2). Sometimes, pinacoid faces can be found. The average Er and Yb effective distribution coefficient is 0.84 as a consequence of minor differences in the sizes of Y<sup>3+</sup>, Er<sup>3+</sup> and Yb<sup>3+</sup> cations. Yb and Er were uniformly distributed in the grown layers.

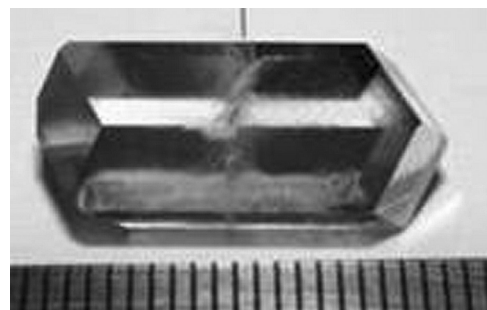


Fig. 2. (Er,Yb):YAB crystal grown by DSSG method.

100  $\mu\text{m}$ -thick Yb:YAB single crystal layers were obtained on  $(10\bar{1}1)$ -oriented YAB substrates. Average growth rates were estimated to be within the range of 1.5–10  $\mu\text{m}/\text{mm}$  under supercoolings up to 3–12.5  $^{\circ}\text{C}$  (Fig. 3). Excess of rare earth oxides in the system possessed to decrease growth rates of this surfaces. The surface morphology was quite good and flat over large areas. There were no visible solution inclusions in the layers, nevertheless some cracks could be identified.

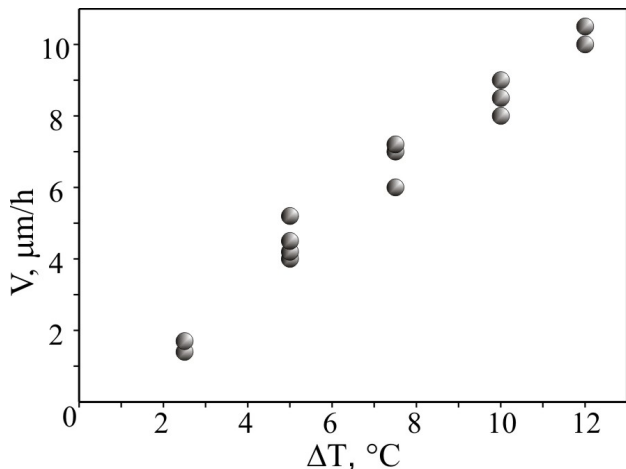


Fig. 3. Normal growth rate of Yb:YAB films vs. supercooling of solution.

### 3.2. Spectroscopy and laser experiments

From the spectroscopic point of view, (Er,Yb):YAB crystals are characterized by broad Yb absorption band, high nonradiative decay probability and efficient  $\text{Yb}^{3+} \rightarrow \text{Er}^{3+}$  energy transfer. Yb absorption band in Er,Yb:YAB crystal is centered at 976 nm and has the bandwidth of 17 nm FWHM (Fig. 4 a). Fig. 4 b shows absorption and stimulated emission spectra of  $\text{Er}^{3+} 4\text{I}_{13/2} \rightarrow 4\text{I}_{15/2}$  transition that covers the range of 1530–1610 nm. Due to high phonon energies in YAB ( $>1400 \text{ cm}^{-1}$  [21]) the 1.5  $\mu\text{m}$  erbium luminescence is quenched to 325  $\mu\text{s}$  in (Er,Yb):YAB resulting in luminescence quantum yield of about 7%. The lifetime of  $\text{Er}^{3+} 4\text{I}_{11/2}$  level is very short ( $\sim 80 \text{ ns}$ ) thus reducing upconversion and energy back-transfer losses. All this lead to efficient  $\text{Yb}^{3+} \rightarrow \text{Er}^{3+}$  energy transfer (88%) and excellent laser characteristics better than in the best Er,Yb-codoped glasses (up to 1W of cw output power with 35% slope efficiency). Detailed data on spectroscopy and cw lasing in Er,Yb:YAB is published in [13].

The room temperature polarized absorption spectra of 100  $\mu\text{m}$ -thick crystalline layer of  $\text{Yb}^{3+}(10 \text{ at.}\%)$ :YAB on YAB substrate were measured in order to compare with those of Yb:YAB single crystal (Fig. 5). Generally, the spectra are similar, in both samples a strong and broad absorption bands are observed at 976 nm with a peak absorption coefficient of about  $14 \text{ cm}^{-1}$ . Nevertheless

Yb:YAB epitaxial layers exhibit broader spectral bandwidth probably due to influence of the defects in the layer structure. The emission lifetime of  $\text{Yb}^{3+}$  ions in the layer was measured to be 480  $\mu\text{s}$ , the same as in the bulk crystal [13].

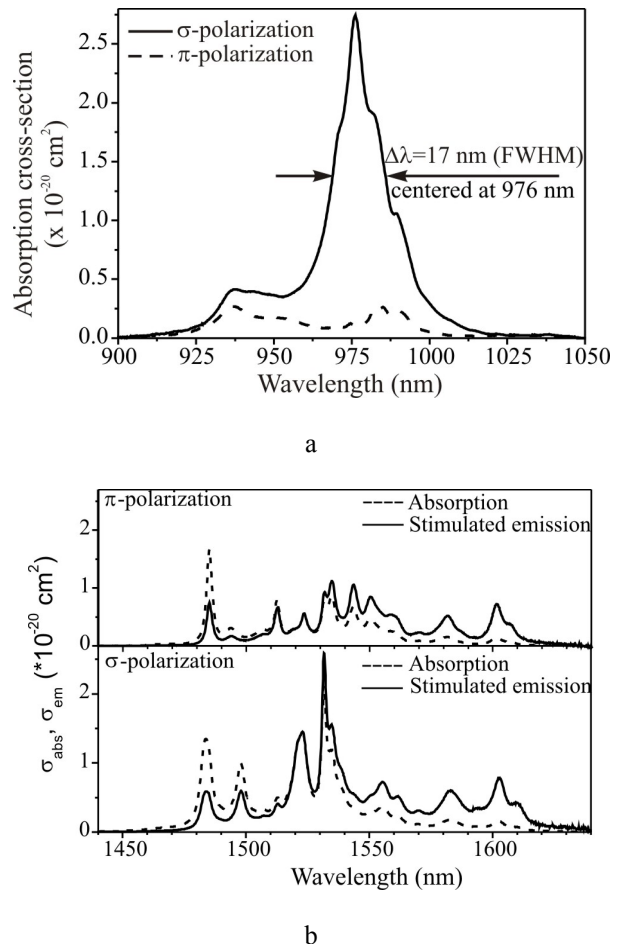


Fig. 4. Absorption and stimulated emission spectra of Er,Yb:YAB crystal at 1  $\mu\text{m}$  (a) and 1.5  $\mu\text{m}$  (b) spectral region.

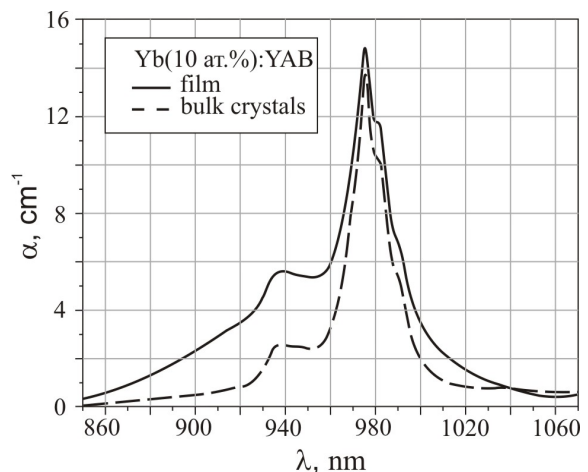


Fig. 5. Ytterbium absorption band at 976 nm of Yb:YAB bulk crystal (dashed line) and crystalline thin film (solid line).

## 5. Conclusions

The visually transparent YAB and (Er,Yb):YAB crystals with a typical size up to  $10 \times 10 \times 15 \text{ mm}^3$  were obtained by the DSSG technique. The average effective distribution coefficient for both  $\text{Er}^{3+}$  and  $\text{Yb}^{3+}$  cations is 0.84. (Er,Yb):YAB single crystals are characterized by broad Yb absorption band centered at 976 nm and short  $\text{Er}^{3+} \text{ } ^4\text{I}_{11/2}$  and  $\text{Yb}^{3+} \text{ } ^4\text{I}_{13/2}$  level lifetimes. This material also exhibit efficient  $\text{Yb}^{3+} \rightarrow \text{Er}^{3+}$  energy transfer (88 %) and excellent laser characteristics exceeded those in the best (Er,Yb)-codoped glasses (up to 1W of cw output power with 35% slope efficiency). 100  $\mu\text{m}$ -thick Yb:YAB single crystalline layers were obtained on  $(10\bar{1}1)$  – oriented YAB substrates. Average growth rates were estimated to be within the range of 1.5–10  $\mu\text{m}/\text{mm}$  for supercoolings varied from 3 to 12.5 °C. Layers obtained exhibit no visible melt inclusions, although some cracks can be observed. The room temperature polarized absorption spectra of a crystalline layer of  $\text{Yb}^{3+}(10\%)$ :YAB on YAB substrate for  $\sigma$ -polarization were measured in order to compare with Yb:YAB single crystal (Fig. 4). The spectra obtained are similar, in both samples a strong and broad absorption bands are observed at 976 nm with a peak absorption coefficient of about  $14 \text{ cm}^{-1}$ . The emission lifetime of  $\text{Yb}^{3+}$  ions in both layers and bulk crystals is about 480  $\mu\text{s}$ .

## Acknowledgement

This research was supported by the grants of RFBR ## 07-05-00680, 08-05-12038\_ofi and 08-05-90010\_bel.

## References

- [1] B. Denker, V. Osiko, B. Galagan, S. Sverchkov, G. Karlsson, F. Laurell, J. Tellefsen, Advanced Solid State Lasers 2002 Conference, Quebec City, Canada, Technical Digest, TuB5, (2002).
- [2] G. J. Spühler, L. Krainer, E. Innerhofer, R. Paschotta, K. J. Weingarten, U. Keller, Opt. Lett. **30**, 263 (2005).
- [3] T. Schweizer, T. Jensen, E. Heumann, G. Huber, Opt. Commun. **118**, 557 (1995).
- [4] B. Simondi-Teisseire, B. Viana, A. M. Lejus, J. M. Benitez, D. Vivien, C. Borel, R. Templier, C. Wyon. IEEE J. Quantum Electron. **QE-32**, 2004 (1996).
- [5] N. A. Tolstik, A. E. Troshin, S. V. Kurilchik, V. E. Kisel, N. V. Kuleshov, V. N. Matrosov, T. A. Matrosova, M.I. Kupchenko. J. Appl. Phys. B **86**, 275 (2007).
- [6] A. Diening, E. Heumann, G. Huber, O. Kuzmin. Conference on Lasers and Electro-Optics, OSA Technical Digest Series 299 (1998).
- [7] N. V. Kuleshov, A. A. Lagatsky, A. V. Podlipensky, V. P. Mikhailov, A. A. Kornienko, E. B. Dunina, S. Hartung, G. Huber. J. Opt. Soc. Am. B **15**, 1205 (1998).
- [8] P. Burns, J. Dawes, P. Dekker, J. Piper, H. Jiang, J. Wang. J. Quantum Electron **40**, 1575 (2004).
- [9] B. Denker, B. Galagan, L. Ivleva, V. Osiko, S. Sverchkov, I. Voronina, J. E. Hellstrom, G. Karlsson, F. Laurell. J. Appl. Phys. B **79**, 577 (2004).
- [10] P. Dekker, J.M. Dawes, J.A. Piper, Y. Liu, J. Wang. Opt. Commun. **195**, 431 (2001).
- [11] D. Jaque, J. Capmany, J.G. Sole. Appl. Phys. Let. **75**, 325 (1999).
- [12] W. You, Y. Lin, Y. Chen, Z. Luo, Y. Huang. J. Cryst. Growth **270**, 481 (2004).
- [13] N. A. Tolstik, S. V. Kurilchik, V. E. Kisel, N. V. Kuleshov, V.V. Maltsev, O. V. Pilipenko, E. V. Koporulina, N. I. Leonyuk. Opt. Lett. **32**, 3222 (2007).
- [14] A. A. Lagatsky, V. E. Kisel, A. E. Troshin, N. A. Tolstik, N. V. Kuleshov, N. I. Leonyuk, A. E. Zhukov, E. U. Rafailov, W. Sibbett, Optics Letters **33**, 83 (2008).
- [15] V. Petrov, F. Guell, J. Massons, J. Gavalda, R. M. Sole, M. Aguilo, F. Diaz, U. Griebner, IEEE Quantum Electron. **40**, 1244 (2004).
- [16] U. Griebner, J. Lui, S. Rivier, A. Aznar, R. Grunwald, R. M. Sole, M. Aguilo, F. Diaz, V. Petrov. IEEE Quantum Electron. **41**, 408 (2005).
- [17] Y. E. Romanyuk, C. N. Borca, M. Pollnau, S. Rivier, V. Petrov, U. Griebner. Conference on Lasers and Electro-Optics/Europe-2005, Munich, Germany, Tech. Digest., CJ6-3-THU (2005).
- [18] J. L. Blows, P. Dekker, P. Wang, J. M. Dawes, T. Omatsu, Appl. Phys. B **76**, 289 (2003).
- [19] N. I. Leonyuk, L. I. Leonyuk. Prog. Crystal Growth and Charact. **31**, 179 (1995).
- [20] V. V. Filippov, I. T. Bondar', N. V. Kuleshov, N. I. Leonyuk, V. V. Mal'tsev, O. V. Pilipenko. J. Opt. Technol. **74**, 717 (2007).
- [21] D. Jaque, M.O. Ramirez, L.E. Bausa, J.G. Sole, E. Cavalli, A. Spaghini, M. Betinelli. Phys. Rev. B **68**, 035118 (2003).

\*Corresponding author: leon@geol.msu.ru